Supplemental Materials

Molecular Biology of the Cell

Sobolik et al.

Supplementary Materials and Methods

Reagents and Inhibitors

CXCL12 (PeproTech) was dissolved in 0.1% BSA (bovine serum albumin) in sterile water. AMD3100 (an inhibitor of CXCR4, Tocris Biosciences), PD98059 (an inhibitor of MEK1, Cell Signaling), Ly294002 (an inhibitor of PI3K, Cell Signaling), U0126 (an inhibitor of MEK1/2, Promega), SB265610 (a CXCR2-specific antagonist, GSK Pharmaceuticals), and CCX771 (a CXCR7-specific antagonist, a kind gift from ChemoCentryx, Mt View, CA) were each separately dissolved in dimethyl sulfoxide (DMSO). Cells were incubated at indicated time points in the figure legends in 3D rBM cultures in the presence of control (DMSO), PD98059 (20 μM) and AMD3100 (40 μM), U0126 (10 μM) and SB265610 (1 μM), or CCX771 (1 μM) alone. For combined treatment, cells were incubated in 3D rBM cultures in the presence of control (DMSO), Ly294002 (2 μM) and PD98059 (10 μM), Ly294002 (2 μM) and U0126 (10 μM), Ly294002 (2 μM) and AMD3100 (20 μM), U0126 (10 μM) and AMD3100 (20 μM), or PD98059 (10 μM) and AMD3100 (20 μM). SB265610 and CCX771 were used at 1 μM for all combinational experiments. All inhibitors were added to the medium on alternate days.

Western Blot

Cell lysis and western blot analysis were performed as previously described (5). Antibodies against E-cadherin (4A2), N-cadherin (13A9), and β-catenin (15B8) were gifts from Dr. James Wahl (University of Nebraska Medical Center, Lincoln, Nebraska). Other antibodies used were against p120/pp120 (BD biosciences), cadherin 11 (Sigma), ZEB-1 (Santa Cruz), active MAPK (Cell Signaling), ERK2 (Santa Cruz), pAKT473 (Cell Signaling), pan-AKT (Cell Signaling), and tubulin (Sigma). Proteins were visualized either by enhanced chemiluminescence (Pierce) or by scanning the emitted IR spectrum from Alexa dye-conjugated secondary antibodies (Molecular Probes) using the Odyssey System (LI-COR Biotechnology).

Western blot of cells from 3D rBM cultures

Cells were lysed in RIPA buffer containing protease and phosphatase inhibitors. The Matrigel matrix and acini were collected and pulled through a 22-gauge needle 3–5 times. The lysate was spun at 15,000 *x g* at 4°C for 15 minutes, the supernatant collected, and the CytoTox 96 assay (Promega) used to measure lactate dehydrogenase activity for lysate normalization. Western blotting was performed as above.

Immunofluorescence

Cells were immunostained as described previously (2). The primary antibodies used were anti-E-cadherin, anti-β-catenin, anti-p120, anti-cadherin 11, anti-ZEB-1, and anti-CXCR4 (MAB 170, R&D Systems)**.** Proteins were visualized with appropriate Cy3-conjugated secondary antibodies (Jackson Labs). Immunofluorescence staining for co-localization of cadherin 11 (mouse monoclonal) and p120 (rabbit polyclonal, kind gift from Dr. Albert Reynolds, Vanderbilt University Medical Center, Nashville, Tennessee) and cadherin 11 (mouse monoclonal) and β-catenin (rabbit polyclonal) were incubated with species specific Cy3- and Cy5-conjugated secondary antibodies. Proteins were visualized with appropriate Cy3 or Cy5-conjugated secondary antibodies (Jackson Labs). Staining was visualized using a Zeiss Axioplan 2 microscope equipped with a Hamamatsu Orca ER fluorescent camera or an LSM 510 META inverted confocal microscope with a 40X/1.3 plan apochromat objective. Images were processed using MetaMorph software (Molecular Devices). Co-localization of cadherin 11 with p120 and cadherin 11 with β-catenin was quantified using Metamorph Imaging System software package (Molecular Devices Corporation). Threshold levels for all images were kept consistent among all images. Images were taken from four fields of view in two separate experiments. The percent co-localization is indicative of the area of cadherin 11 and stained fluorescent pixels overlapping that of p120 or β-catenin.

Transwell Invasion Assays

Invasion assays were performed using matrigel coated transwell chambers with 8 μm pores according to the manufacturer's instructions (BD Biosciences). MCF-7 Vector, MCF-7 CXCR4WT, MCF-7 CXCR4ΔCTD, or MDA-MB-231 cells were suspended at 2 X 10^4 cells/ml in serum-free medium in the upper chamber of a 24-well cell culture insert. Then, serum free media with 100 ng/ml of CXCL12 or 100 ng/ml of CXCL12 with 20 uM of AMD3100 was added to the lower chamber. The chambers were incubated for 24 hr at 37°C in 5% CO_2. After 24 hr, the top of the filter was scraped with cotton swabs to remove the cells that did not migrate to the bottom of the well. Cells on the bottom of the filter were stained with Diff-Quick stain set (Dade Diagnostic, Inc.). Cells on the underside of the filters were examined and counted under a microscope. Each cell line was plated in triplicate, and each experiment was repeated three times. Five random fields of cells from each filter were counted at 10x magnification. The average number of cells in a field was calculated and the average of these values over the triplicate wells was the unit of analysis. Data were depicted in barplots as the mean (+standard deviation). MCF-7 vector control versus MCF-7 CXCRWT or MCF-7 CXCR4ΔCTD groups were compared using the two-sample *t* test. P-values <0.017 were considered statistically significant following the Bonferroni correction to control the experiment-wise error rate below 5%.

Zymography analysis

Functional activity of MMP-2 and MMP-9 were evaluated by gelatin zymography as described previously (6) ENREF 37 ENREF 37 ENREF 38. Proteolytic activities of latent and activated gelatinases were visualized as clear bands against the blue background of stained gelatin, with a molecular mass of 72 and 62 kDa, respectively.

Supplementary Figure Legends

Supplementary Figure 1. Expression of CXCR4ΔCTD in MCF-7 breast carcinoma cells results in p120 isoform switching and up-regulation of vimentin..

(a) Phase contrast images of MCF-7 cells expressing CXCR4 wild-type (WT) or the CXCR4 truncated mutant (CXCR4ΔCTD). Bars, 150 μm. (b) Western blot of E-cadherin, N-cadherin, β-catenin, and tubulin (loading control). (c) Immunofluorescence staining of E-cadherin, β-catenin, and p120. Bars, 150 μm. (d) Western blot of p120 isoforms (indicated with arrows) and tubulin in MCF-7, MCF-7 vector control, MCF-7 CXCR4WT, MCF-7 CXCR4ΔCTD, and MDA-MB-231 cells. (e) Western blot of vimentin and tubulin. (f) Immunofluorescence staining of vimentin. Bars, 150 μm.

Supplementary Figure 2. Inhibition of CXCR4 decreases invasion of MCF-7CXCR4WT and MDA-MB-231 cells, but not MCF-7 CXCR4ΔCTD cells.

(a) Effects of CXCL12 on invasion of breast cancer cells. Invasion assays were performed using transwell filters coated with Matrigel. 2×10^4 cells were plated in serum free media in the top chamber chamber while serum free media with 100 ng/ml of CXCL12 was added to the lower chamber and the culture was allowed to incubate for 24 hours. Cells that transversed the membrane were stained and counted. The columns on the graph represent mean values of three independent experiments while the bars represent the standard deviation.
(b) Effects of AMD3100 on invasion of breast cancer cells. Invasion assays were performed using transwell filters coated with Matrigel. 2×10^4 cells were plated in serum free media in the top chamber while serum free media with 20 uM of AMD3100 was added to the lower chamber and the culture was allowed to incubate for 24 hours. Cells that transversed the membrane were

stained and counted. The columns on the graph represent mean values of three independent experiments while the bars represent the standard deviation. MDA-MB-231 cells are a CXCR4+ cell line used as a control.

(c) Effects of AMD3100 in the presence of CXCL12 stimulation on invasion of breast cancer cells. Invasion assays were performed using transwell filters coated with Matrigel. 2 X 10^4 cells were plated in serum free media in the top chamber chamber while serum free media with 100 ng/ml of CXCL12 and 20 uM of AMD3100 was added to the lower chamber and the culture was allowed to incubate for 24 hours. Cells that transversed the membrane were stained and counted. The columns on the graph represent mean values of three independent experiments while the bars represent the standard deviation.

Supplementary Figure 3. p120 isoform switching in 2D and 3D rBM cultures, and effects of small-molecule inhibitors on MCF-7 vector control cells, MCF-7 CXCR4WT cells, MCF-7 CXCR4ΔCTD cells, and MDA-MB-231 cells in 2D cultures.

(a) Western blot of p120 and tubulin in cells from 2D compared with 3D rBM cultures at day 12. (b) Cells were serum-starved overnight and treated with CXCL12 (100 ng/ml) at the indicated time points. Western blot analyses were performed for active MAPK (pERK1/2), total ERK, and tubulin (loading control). (c) Western blot analysis of Active MAPK, ERK2, and tubulin from cells grown in 3D rBM cultures at day 10 in the presence of inhibitors as indicated. Densitometric scans from duplicate assays were quantitated and active MAPK was normalized to ERK2.

Supplementary Figure 4. Effects of CXCR4, MEK1/2, MEK1, and PI3K single inhibition on the global composition of CXCR4 expressing cells in 3D rBM.

Histograms depict the average number of cells in treatment groups for (a) MCF-7 CXCR4 WT cells; (b) MCF-7 CXCR4ΔCTD cells; (c) MDA-MB-231 cells in 3D rBM cultures. Cell morphology

was assessed at the indicated time points. The columns on the graph represent mean values of three independent experiments while the bars represent the standard deviation.

Supplementary Figure 5. Effects of CXCR4 and MEK inhibition on the global composition of CXCR4 expressing cells in 3D rBM.

Histograms depict the average number of cells in treatment groups for (a) MCF-7 CXCR4 WT cells; (b) MCF-7 CXCR4ΔCTD cells; (c) MDA-MB-231 cells in 3D rBM cultures. Cell morphology was assessed at the indicated time points. The columns on the graph represent mean values of three independent experiments while the bars represent the standard deviation.

Supplementary Figure 6. Effects of CXCR4, PI3K, and MEK inhibition on the global composition of CXCR4 expressing cells in 3D rBM.

Histograms depict the average number of cells in treatment groups for (a) MCF-7 CXCR4 WT cells; (b) MCF-7 CXCR4ΔCTD cells; (c) MDA-MB-231 cells in 3D rBM cultures. Cell morphology was assessed at the indicated time points. The columns on the graph represent mean values of three independent experiments while the bars represent the standard deviation.

Supplementary Figure 7. Effects of CXCR2 single inhibition and CXCR2 inhibition in combination with CXCR4, PI3K, and MEK inhibition on the global composition of CXCR4 expressing cells in 3D rBM.

Histograms depict the average number of cells in treatment groups for (a) MCF-7 CXCR4 WT cells; (b) MCF-7 CXCR4ΔCTD cells; (c) MDA-MB-231 cells in 3D rBM cultures. Cell morphology

was assessed at the indicated time points. The columns on the graph represent mean values of three independent experiments while the bars represent the standard deviation.

Supplementary Figure 8. Effects of CXCR7 single inhibition and CXCR7 inhibition in combination with CXCR4, PI3K, and MEK inhibition on the global composition of CXCR4 expressing cells in 3D rBM.

Histograms depict the average number of cells in treatment groups for (a) MCF-7 CXCR4 WT cells; (b) MCF-7 CXCR4ΔCTD cells; (c) MDA-MB-231 cells in 3D rBM cultures. Cell morphology was assessed at the indicated time points. The columns on the graph represent mean values of three independent experiments while the bars represent the standard deviation.

Supplementary Figure 9. Expression of E-cadherin in MCF-7 CXCR4ΔCTD cells

(a) Phase contrast images of MCF-7 cells expressing CXCR4 wild-type (CXCR4WT), the truncated CXCR4 mutant (CXCR4ΔCTD), or the truncated CXCR4 mutant with expression of E-cadherin (CXCR4ΔCTD, E-cadherin). Cells were photographed 48 hours after seeding. Bars, 150 μm. (b) Western blot of E-cadherin, β-catenin, p120, cadherin 11, and tubulin. (c) Immunofluorescence staining of E-cadherin, β-catenin, p120, and cadherin 11. Bars, 150 μm. (d) Immunofluorescence staining of ZEB-1**.** Bars, 150 μm.

Supplementary Figure 10. MCF-7 CXCR4ΔCTD, E-cadherin-expressing cells exhibit a stellate phenotype in 3D rBM culture.

(a) and (b) Colony formation of MCF-7 vector cells, MCF-7 CXCR4WT cells, MCF-7 CXCR4 ΔCTD cells, MCF-7 CXCR4ΔCTD cells expressing E-cadherin, MDA-MB-231 cells, and MCF10A cells in 3D rBM culture at day 8 (a) or day 12 (b). Phase contrast images are shown. Bars, 150 μm.

Supplementary Figure 11. The schematic diagram summarizes the mechanistic pathways associated with the EMT transition in MCF-7 CXCR4WT cells cultured in 3D rBM, and MCF-7 CXCR4ΔCTD cells cultured in 2D and 3D rBM, and observed in a xenograft model in athymic nude mice.

Supplementary Table S1. Annotated legend for the customized Raybiotech human cytokine antibody array.

The antibody array description was used to determine the antibody locations on the human array.

Supplementary Material Movie 1 and supplementary material movie 2. GFP-MCF-7 vector cells are not detected *in vivo* in absence of exogenous estrogen. The GFP and Texas Red Channels are shown. Rhodamine dextran ingesting myeloid cells and the vasculature were imaged in the Texas Red Channel. Images were taken every 10 seconds for 20 minutes. Images were acquired with an LSM 510 META inverted confocal microscope with a 20X/0.75 plan apochromat objective. Since there are restrictions on file size, resolution of the movies has been reduced from the original size.

Supplementary Material Movie 3. GFP-MCF-7 CXCR4WT cells migrate in single cells streams towards the vasculature *in vivo*. The GFP and Texas Red Channels are shown. MCF-7 CXCR4WT cells were imaged in the green channel, and rhodamine dextran ingesting myeloid cells and vasculature were imaged in the Texas Red Channel. Myeloid cells that infiltrated the tumor environment are motile. Images were taken every 10 seconds for 20 minutes. Images were acquired with an LSM 510 META inverted confocal microscope with a 20X/0.75 plan apochromat objective. Since there are restrictions on file size, resolution of the movies has been reduced from the original size.

Supplementary Material Movie 4. GFP-MCF-7 CXCR4WT cells migrate in single cells streams towards the vasculature *in vivo* in absence of myeloid cells in the tumor. The GFP and Texas Red Channels are shown. MCF-7 CXCR4WT cells were imaged in the green channel, and the vasculature was imaged in the Texas Red Channel. Myeloid cells were not detected in the tumor. Images were taken every 10 seconds for 20 minutes. Images were acquired with an LSM 510 META inverted confocal microscope with a 20X/0.75 plan apochromat objective. Since there are restrictions on file size, resolution of the movies has been reduced from the original size.

Supplementary Material Movie 5. GFP-MCF-7 CXCR4WT cells are non-migratory in areas of the tumor that lack a vasculature *in vivo*. The GFP and Texas Red Channels are shown. MCF-7 CXCR4WT cells were imaged in the green channel, and the vasculature was imaged in the Texas Red Channel. Myeloid cells were not detected in the tumor. Images were taken every 10 seconds for 20 minutes. Images were acquired with an LSM 510 META inverted confocal microscope with a 20X/0.75 plan apochromat objective. Since there are restrictions on file size, resolution of the movies has been reduced from the original size.

Supplementary Material Movie 6. GFP-MCF-7 CXCR4ΔCTD cells display random migration in areas of the tumor that lack a vasculature *in vivo*. The GFP and Texas Red Channels are shown. MCF-7 CXCR4ΔCTD cells were imaged in the green channel, and the vasculature was imaged in the Texas Red Channel. Myeloid cells were not detected in the tumor. Images were taken every 10 seconds for 20 minutes. Images were acquired with an LSM 510 META inverted confocal microscope with a 20X/0.75 plan apochromat objective. Since there are restrictions on file size, resolution of the movies has been reduced from the original size.

Supplementary Material Movie 7. GFP-MCF-7 CXCR4ΔCTD cells migrate towards blood vessels and metastasize to the lymph nodes.

GFP-MCF-7 CXCR4ΔCTD cells (green), vasculature (red) and differentiated HL60 cells were labeled with DiI Cy5 (blue) and injected into the vasculature via a catheter in the femoral vein. Images were acquired 2 hours after injection of labeled HL60 cells with an LSM 510 META inverted confocal microscope with a 40X/1.3 plan apochromat objective. Since there are restrictions on file size, resolution of the movies has been reduced from the original size.

Supplementary Figure 1 (Richmond)

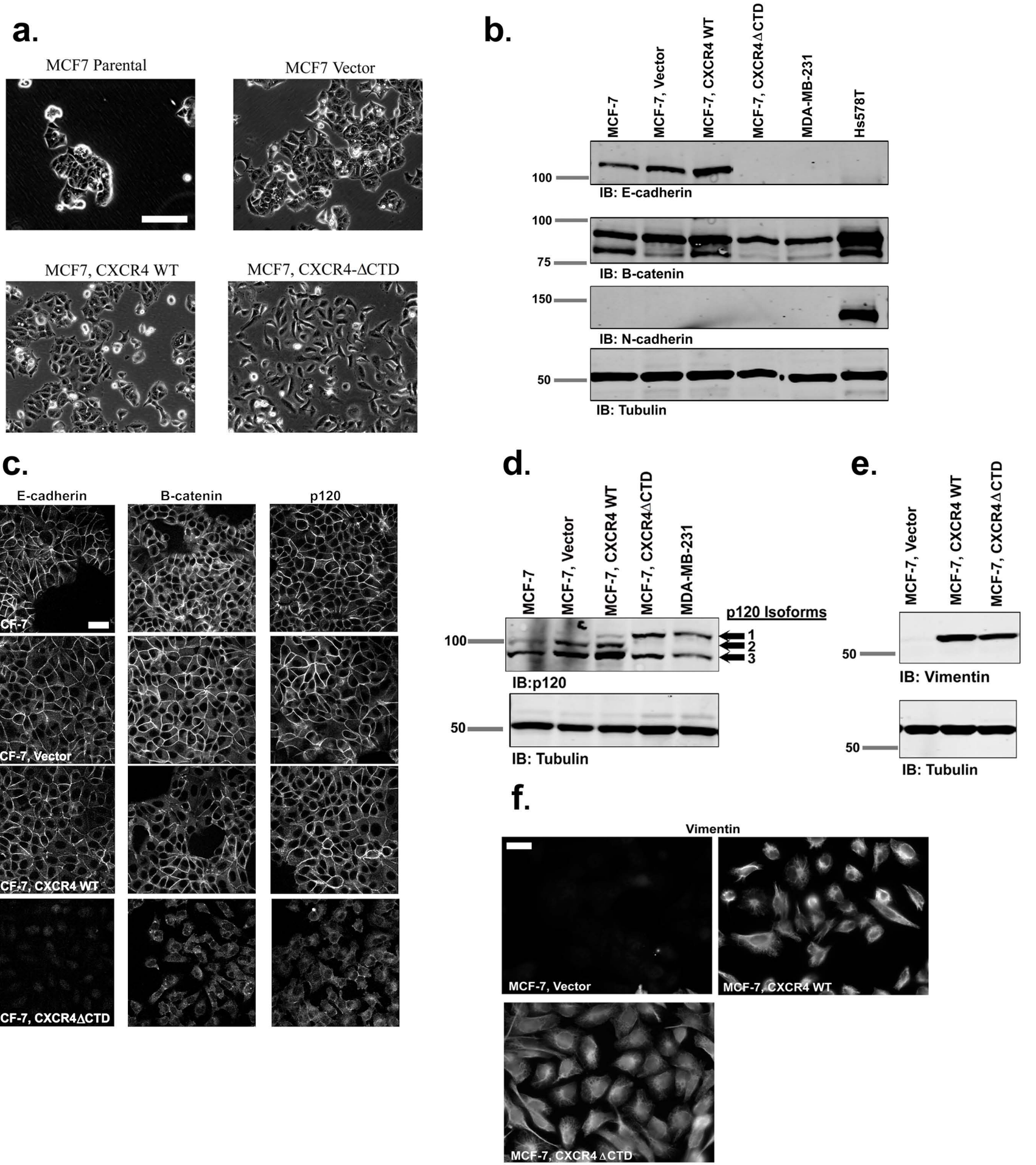

Supplementary Figure 2 (Richmond)

a.

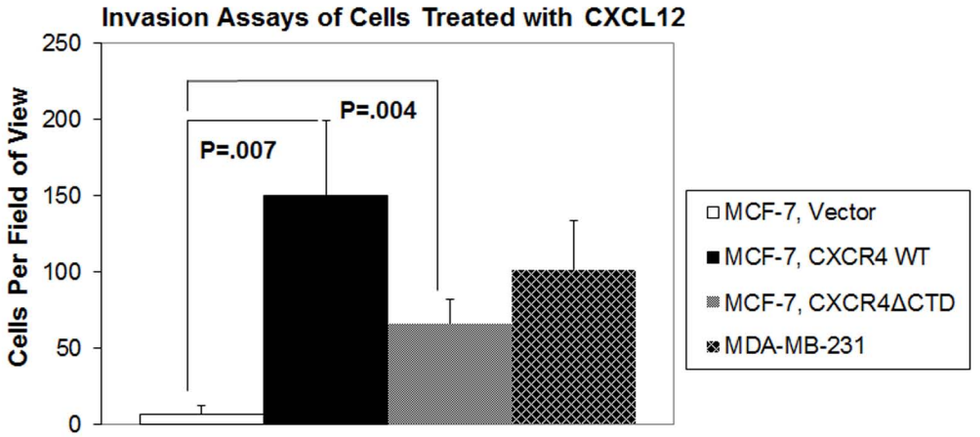

b.

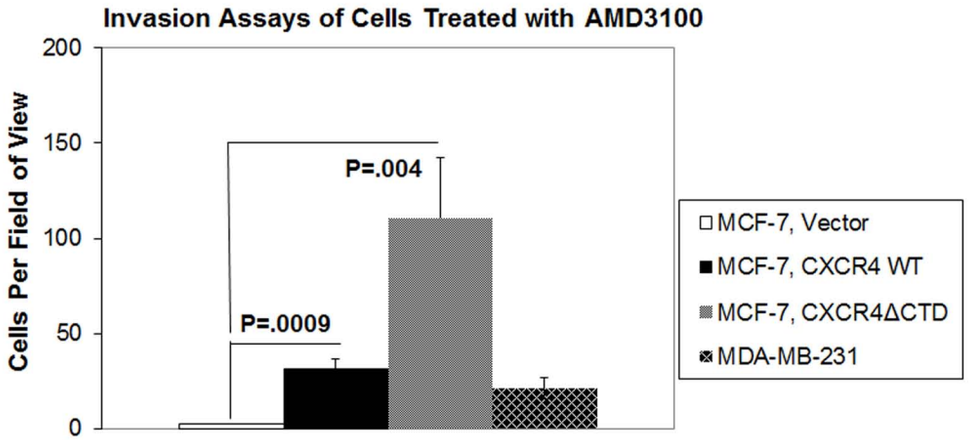

c.

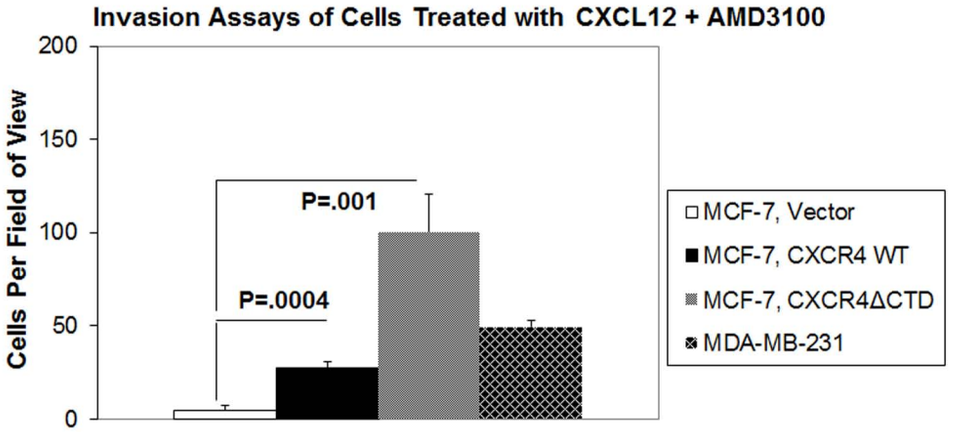

Supplementary Figure 3 (Richmond)

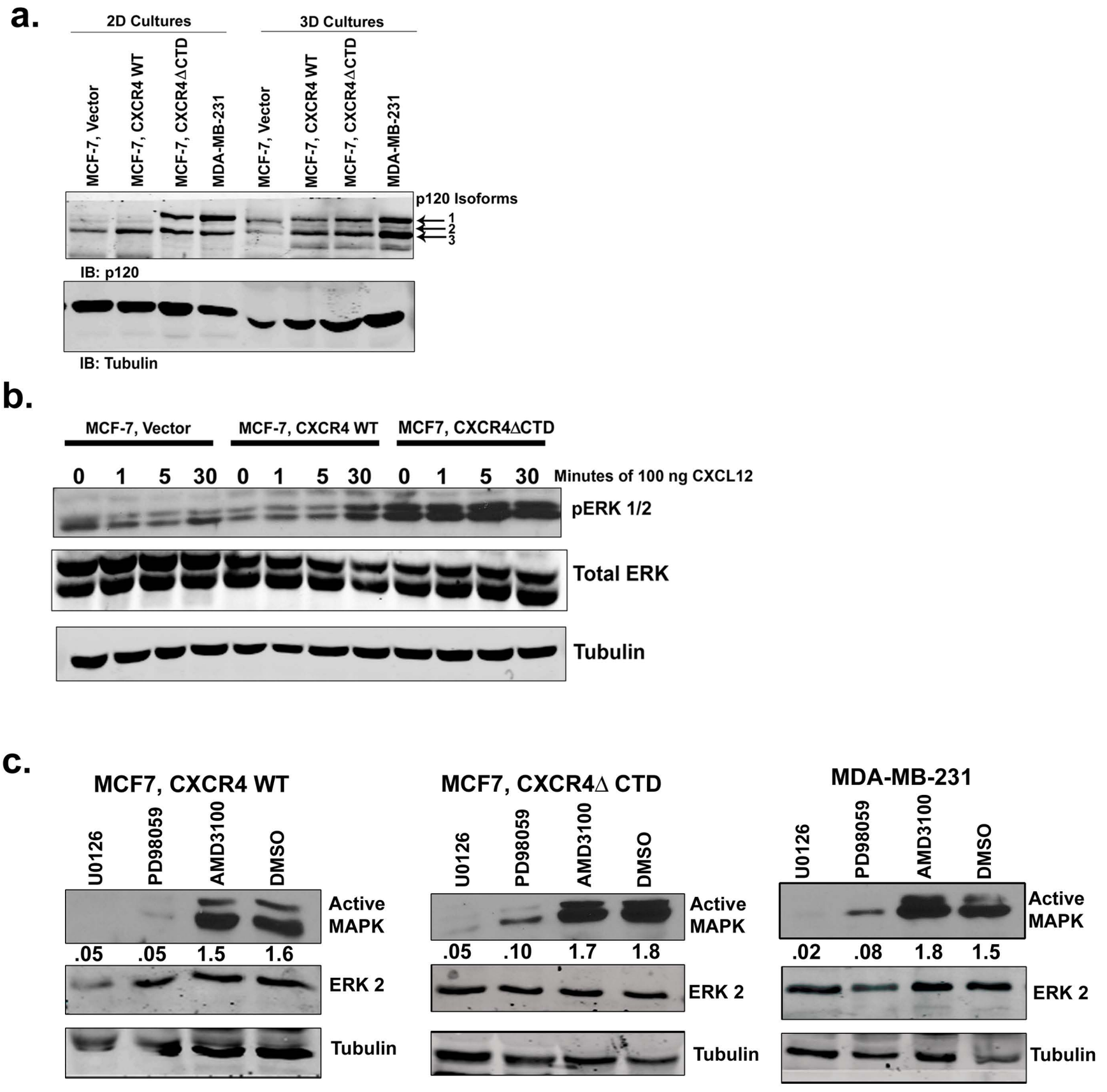

Supplementary Figure 4 (Richmond)

a. MCF-7,CXCR4WT

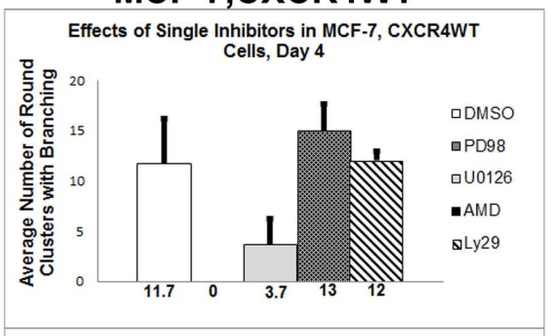

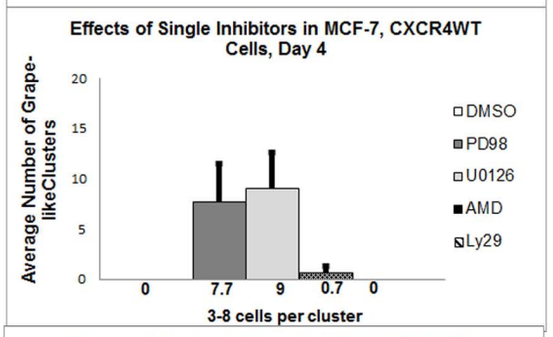

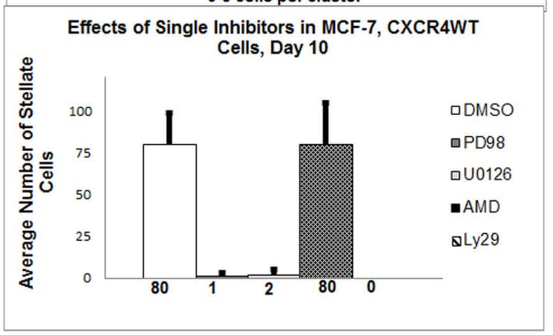

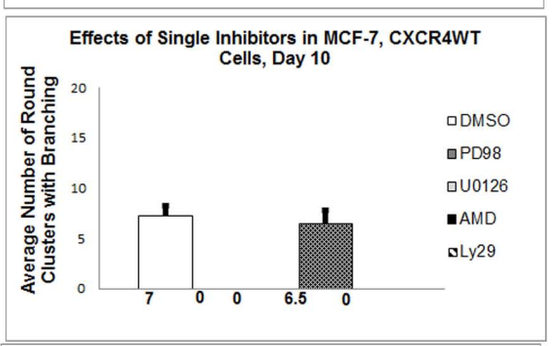

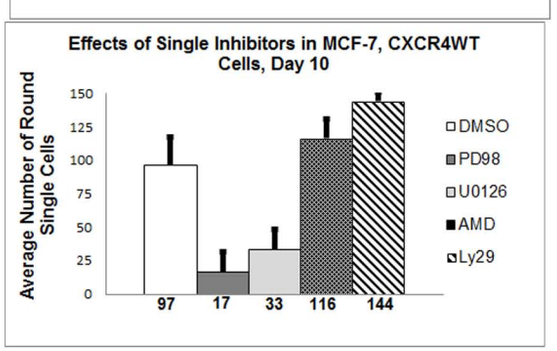

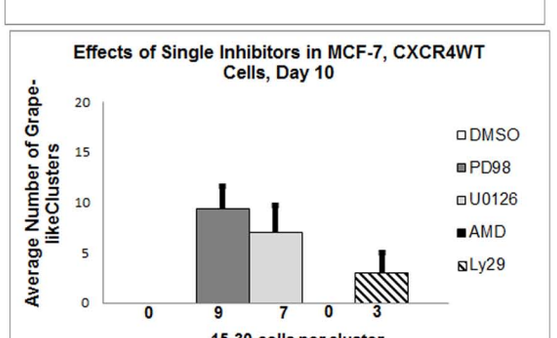

b. MCF-7,CXCR4ΔCTD

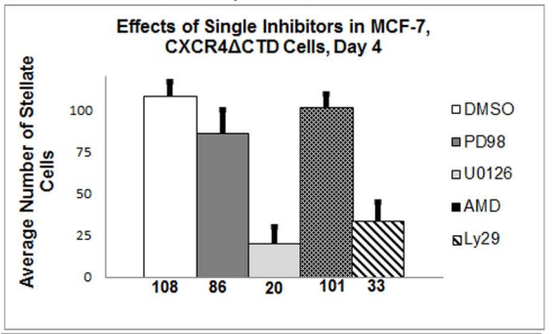

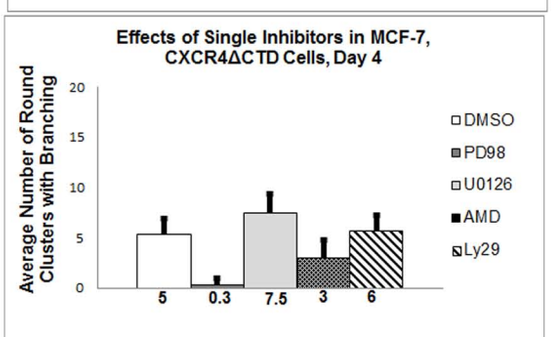

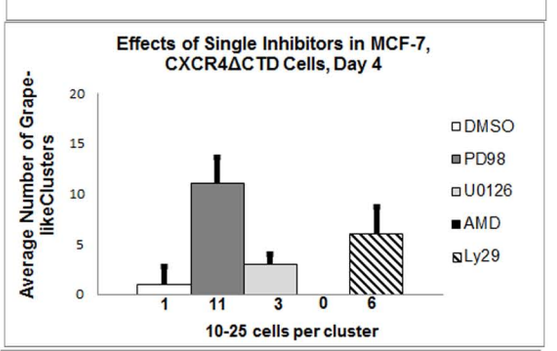

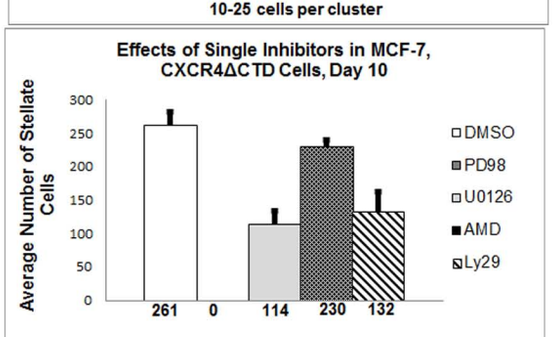

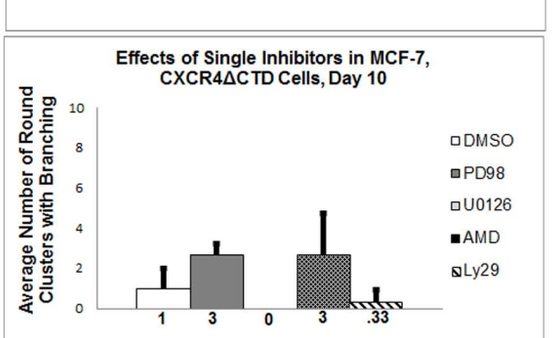

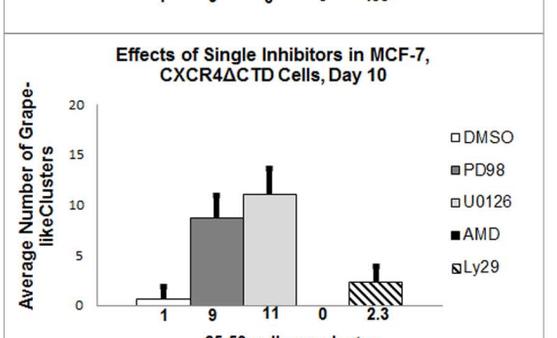

c. MDA-MB-231

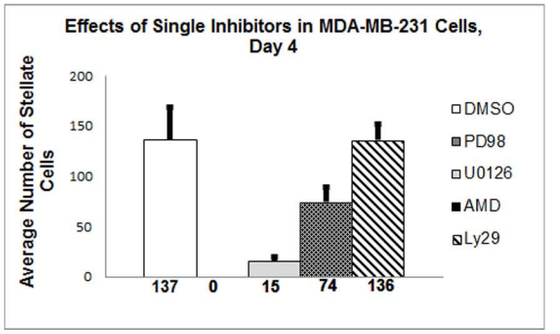

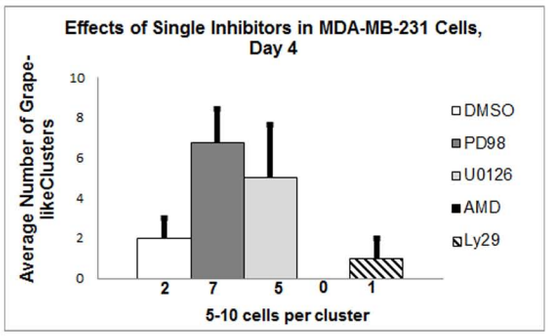

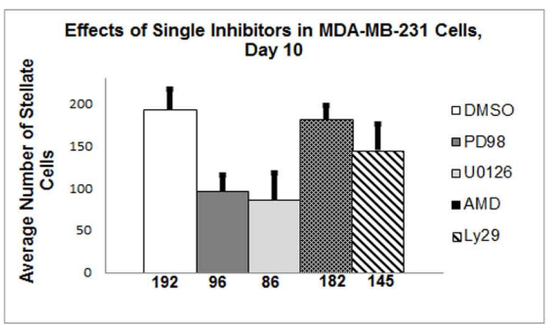

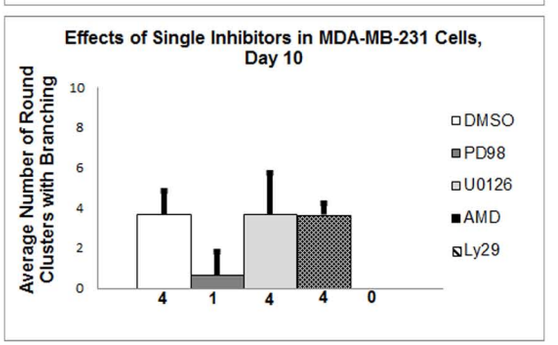

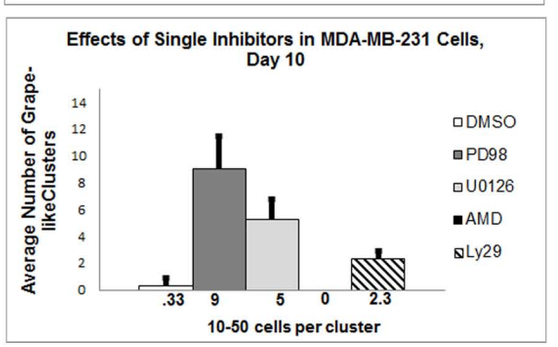

Supplementary Figure 5 (Richmond)

a. MCF-7,CXCR4WT

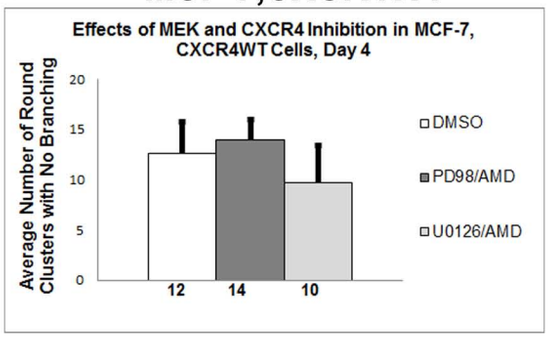

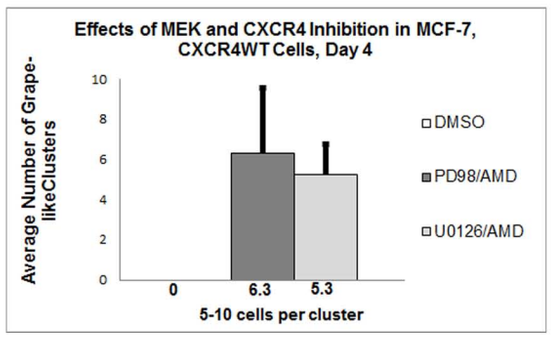

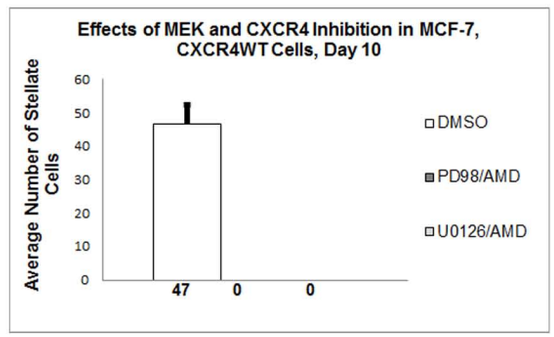

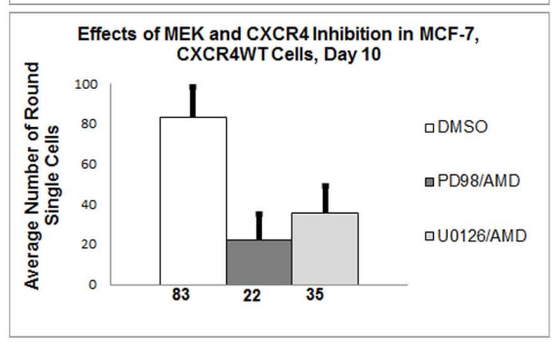

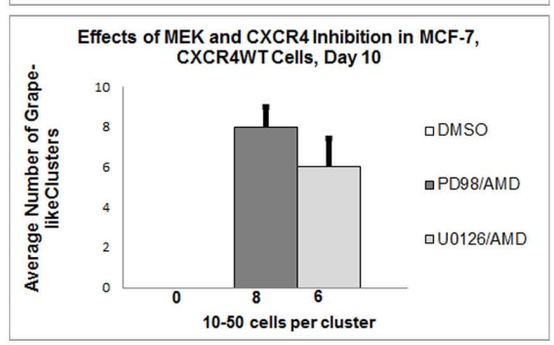

b. MCF-7,CXCR4ΔCTD

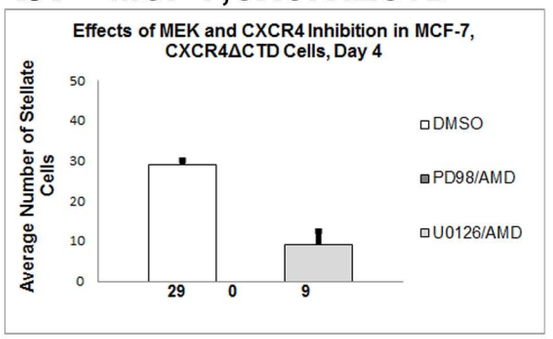

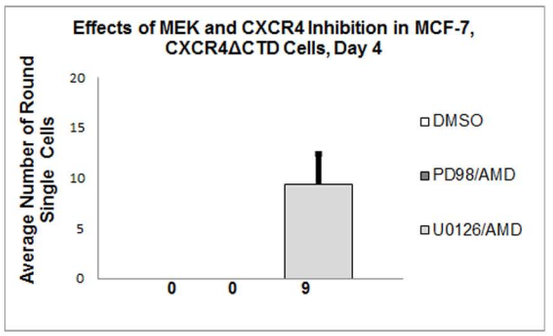

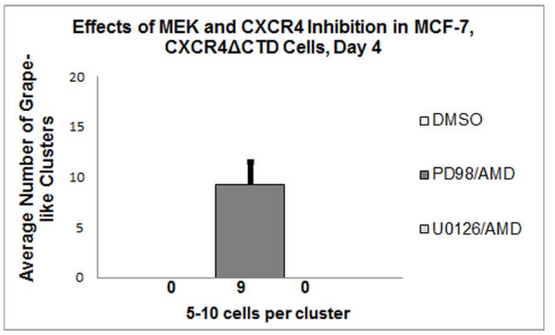

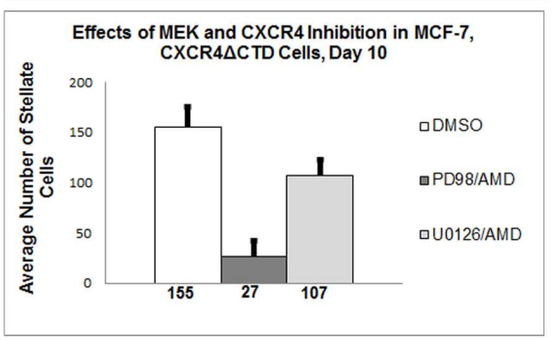

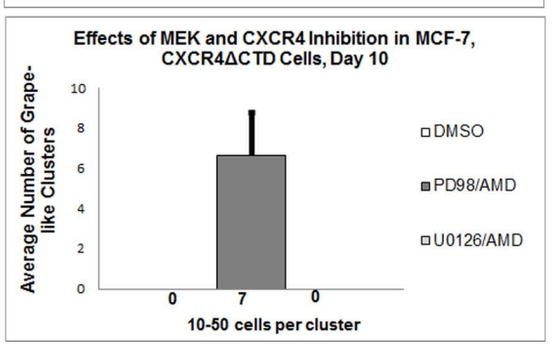

c. MDA-MB-231

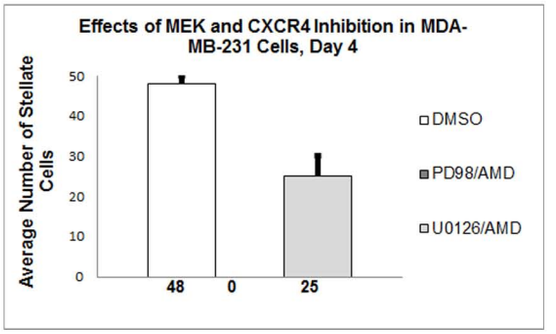

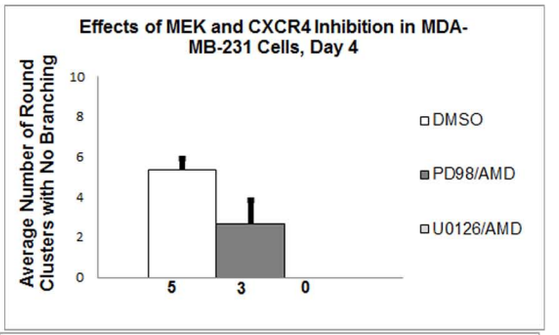

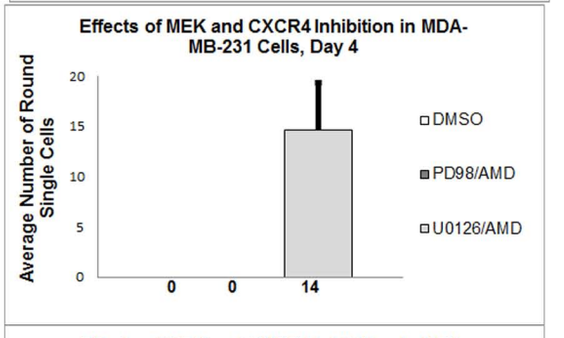

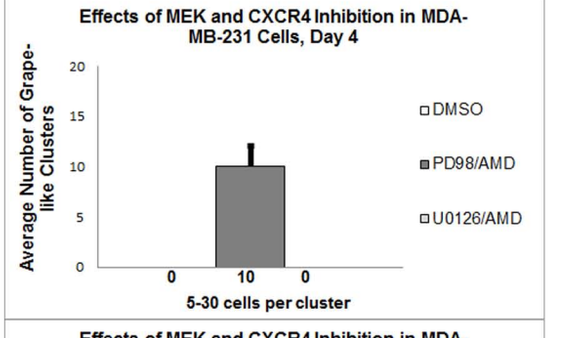

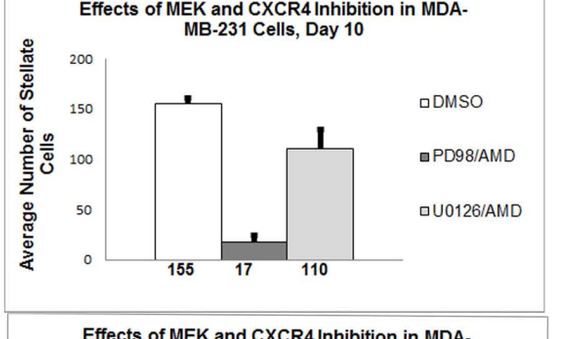

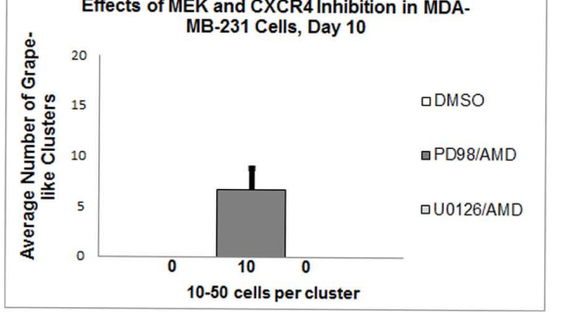

Supplementary Figure 6 (Richmond)

a. MCF-7,CXCR4WT

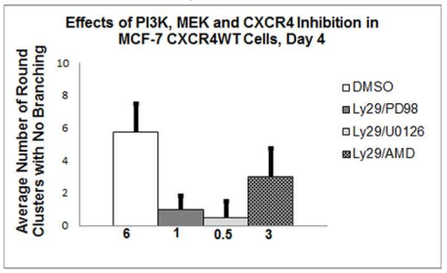

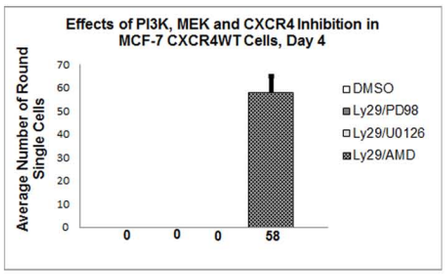

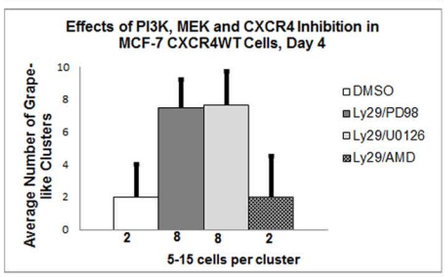

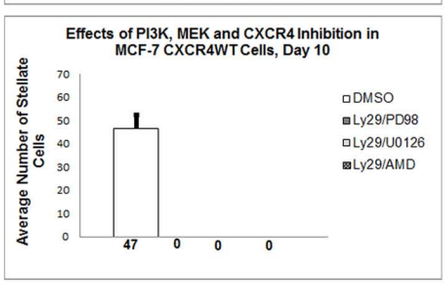

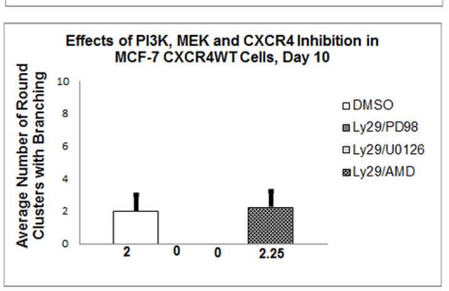

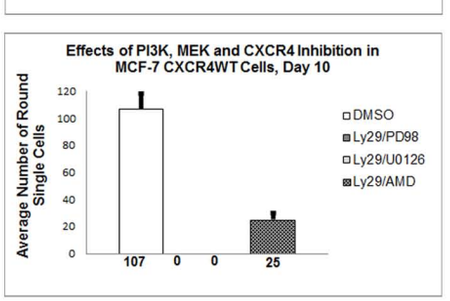

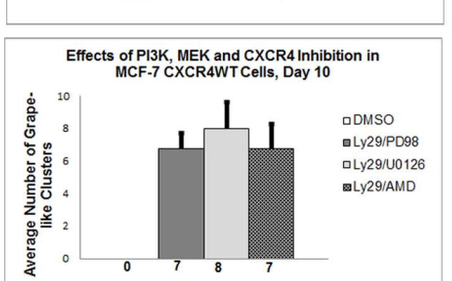

b. MCF-7,CXCR4ΔCTD

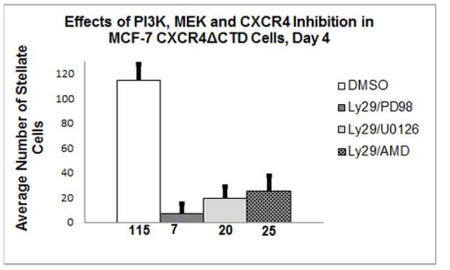

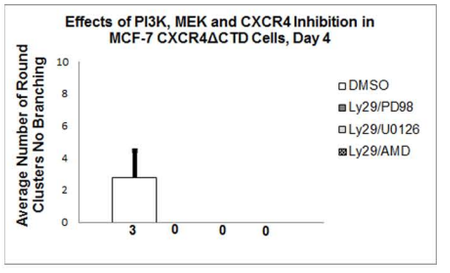

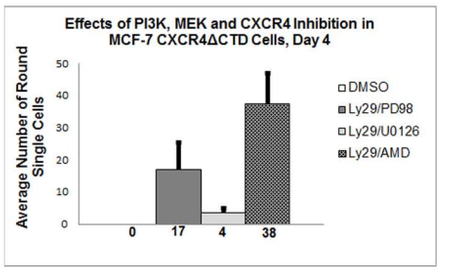

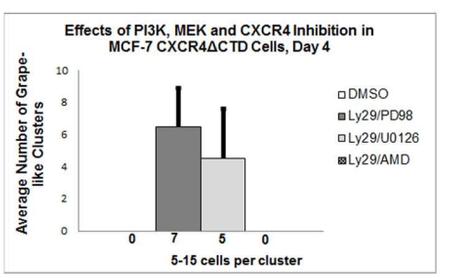

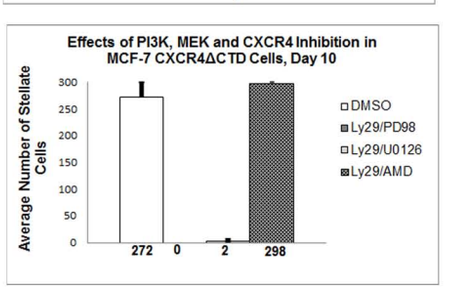

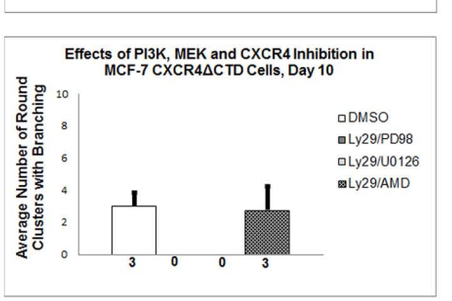

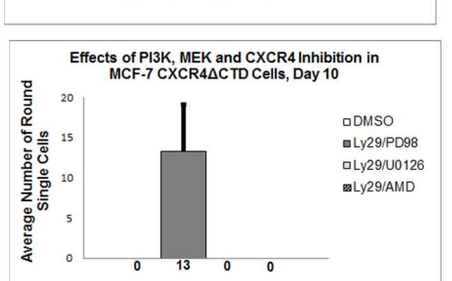

c. MDA-MB-231

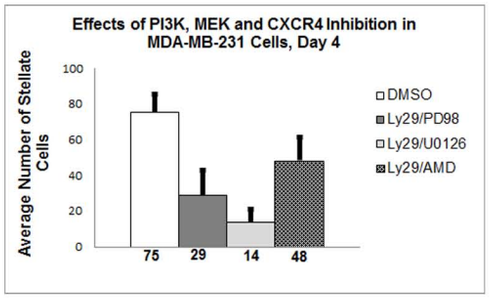

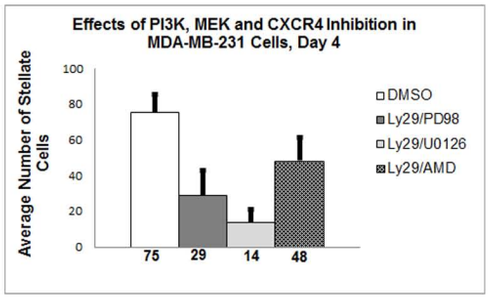

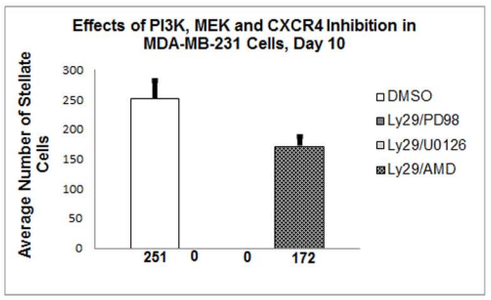

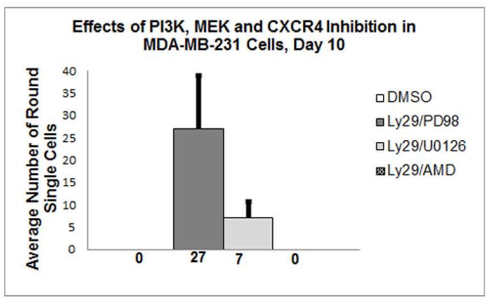

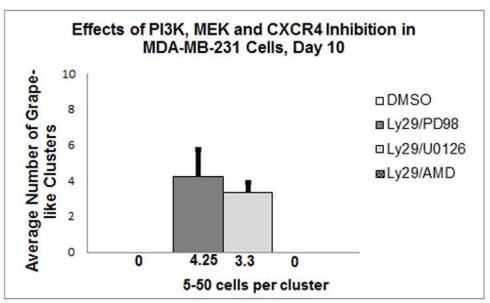

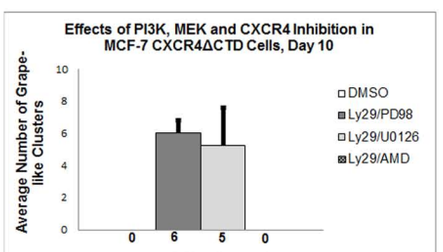

Supplementary Figure 7 (Richmond)

a. MCF-7,CXCR4WT

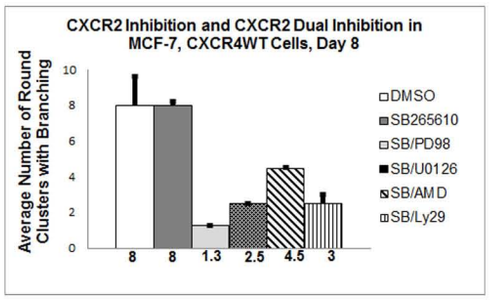

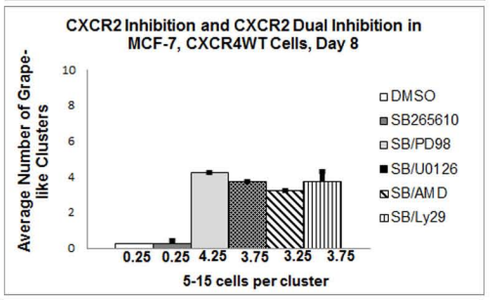

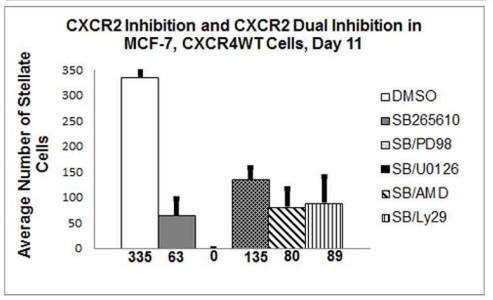

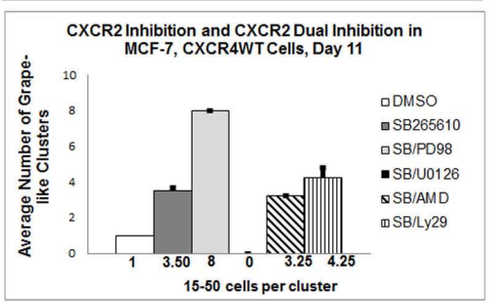

b. MCF-7,CXCR4ΔCTD

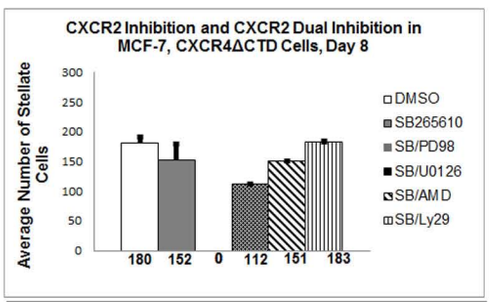

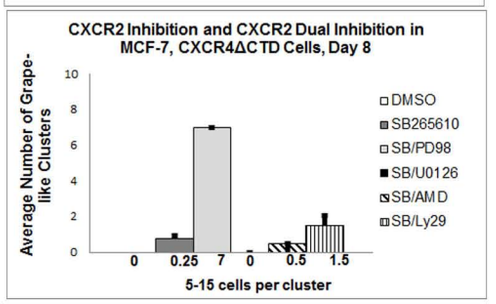

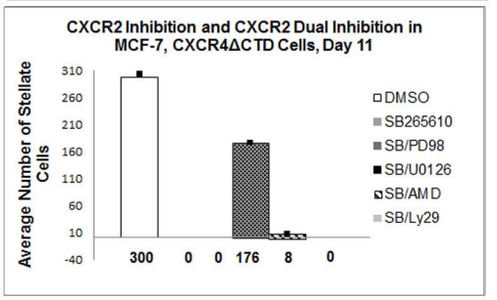

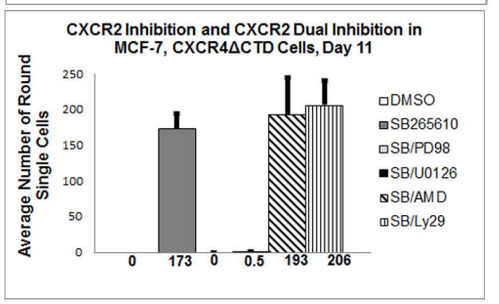

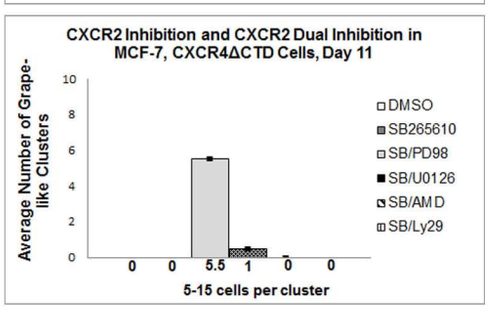

c. MDA-MB-231

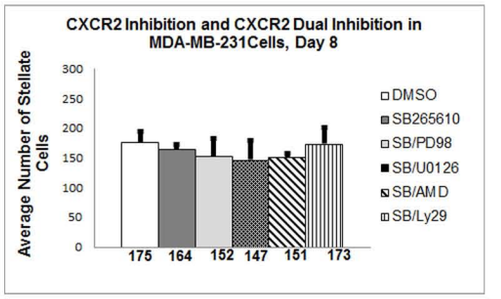

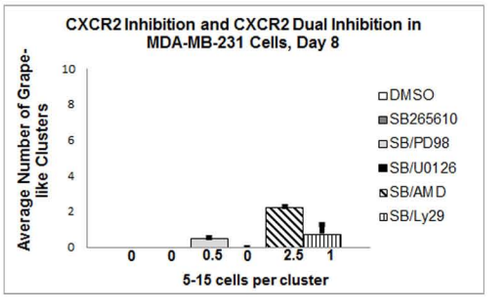

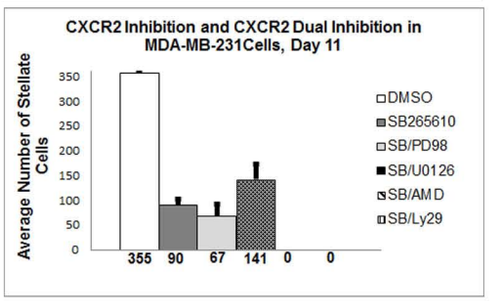

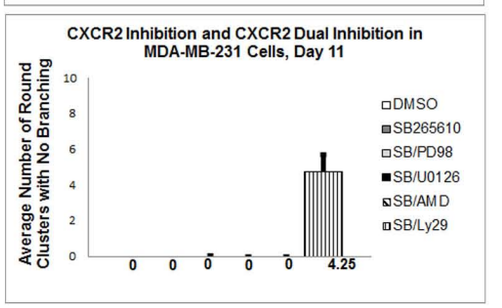

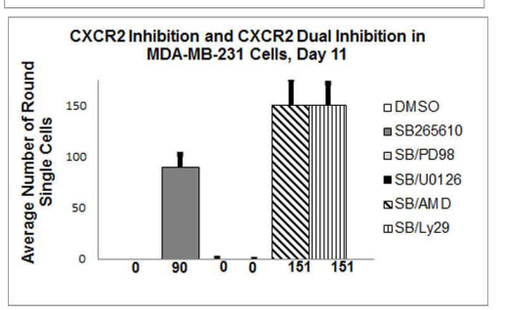

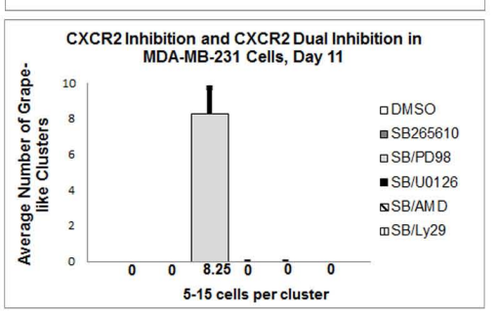

Supplementary Figure 8 (Richmond)

a. MCF-7,CXCR4WT

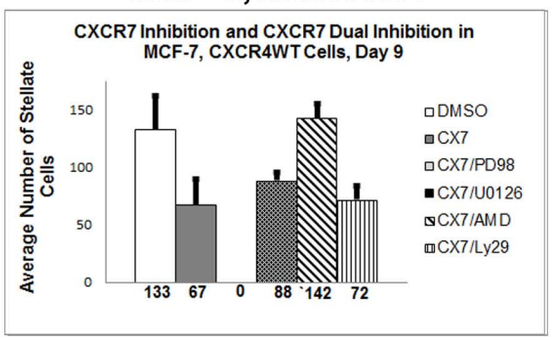

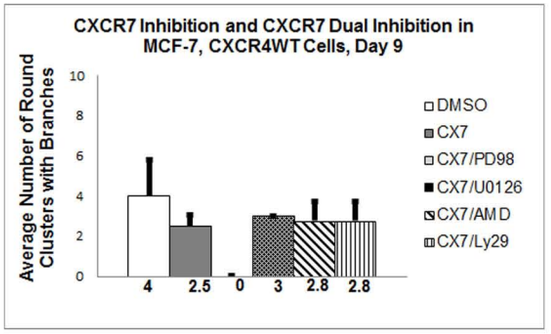

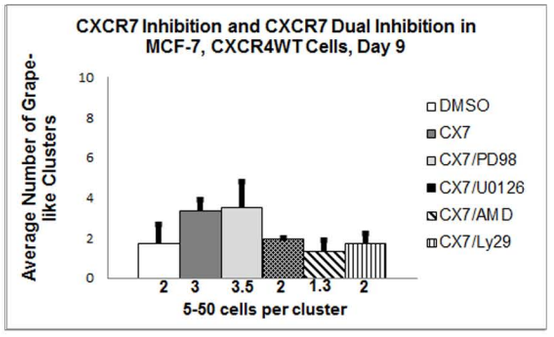

b. MCF-7,CXCR4ΔCTD

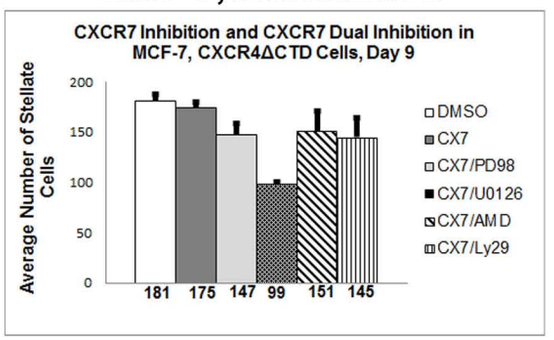

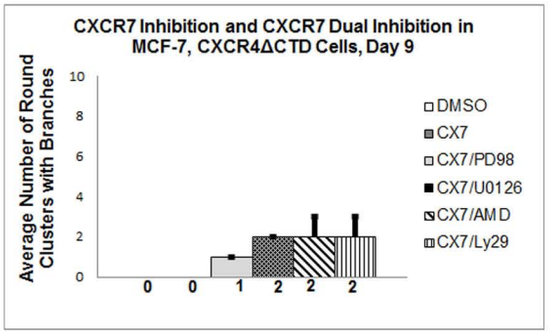

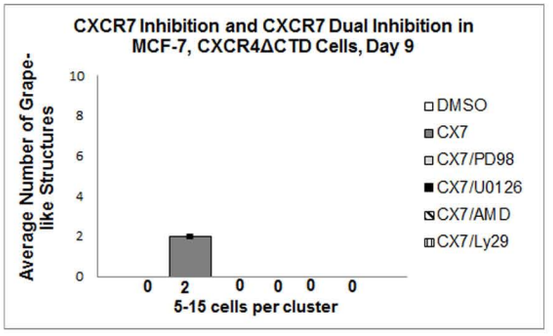

c. MDA-MB-231

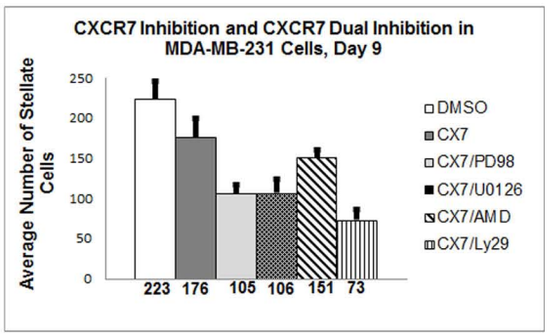

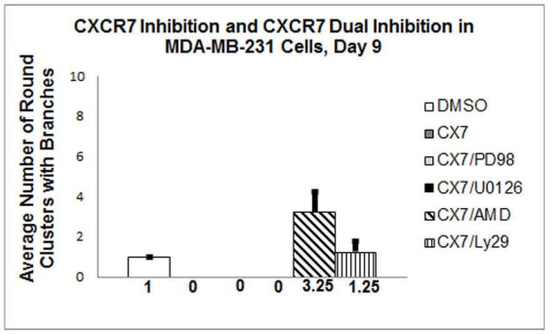

Supplementary Figure 9 (Richmond)

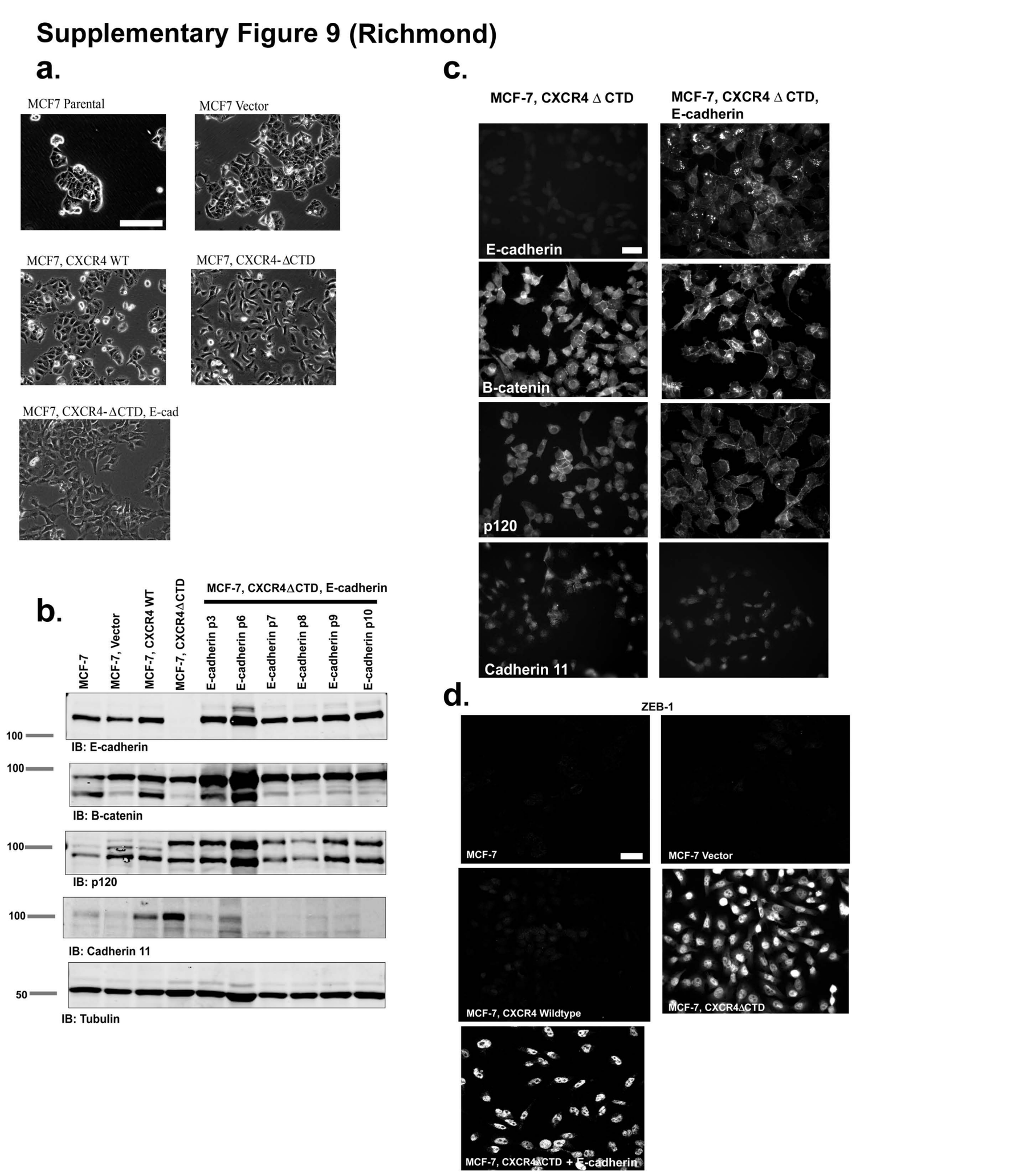

Supplementary Figure 10 (Richmond)

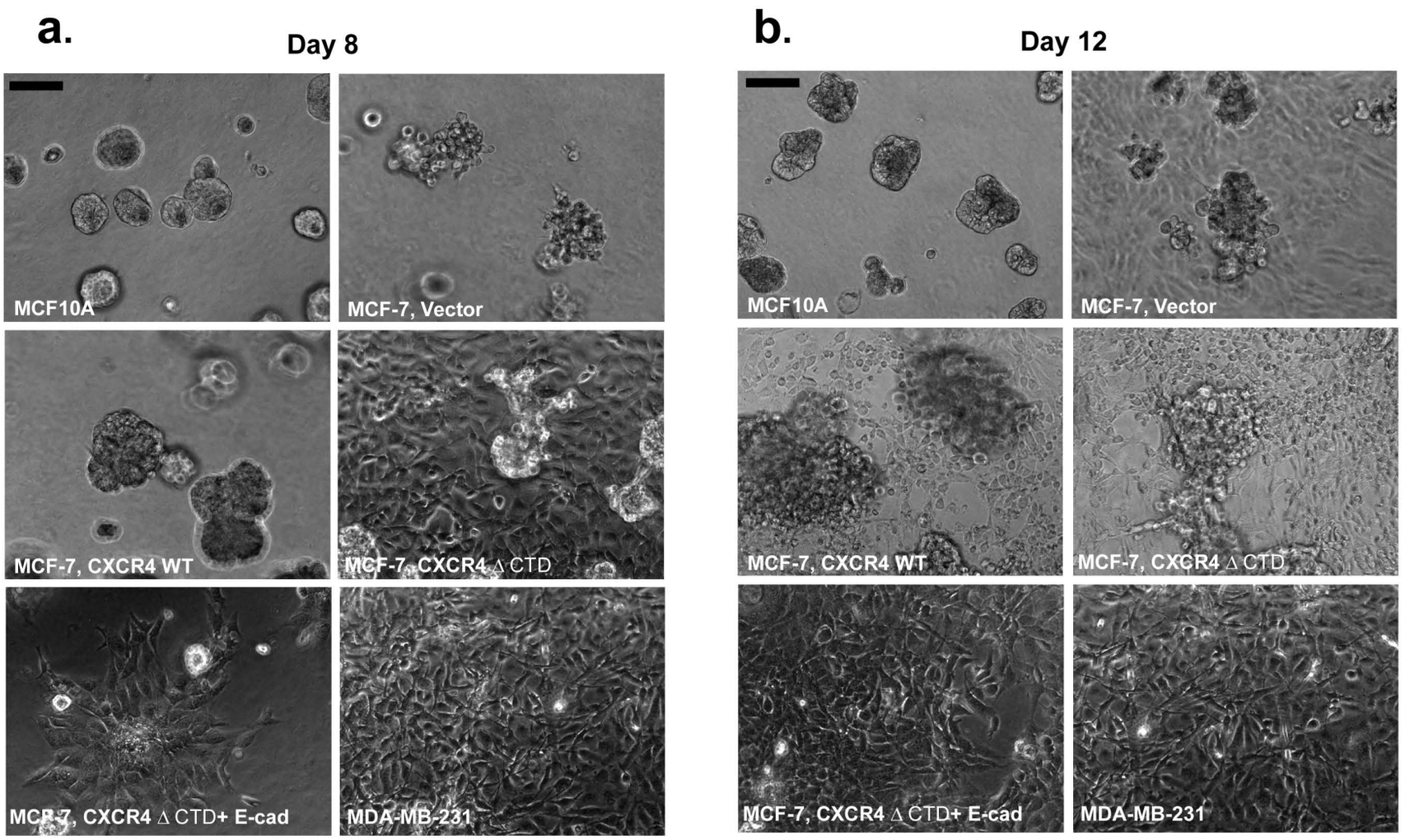

Supplementary Figure 11 (Richmond)

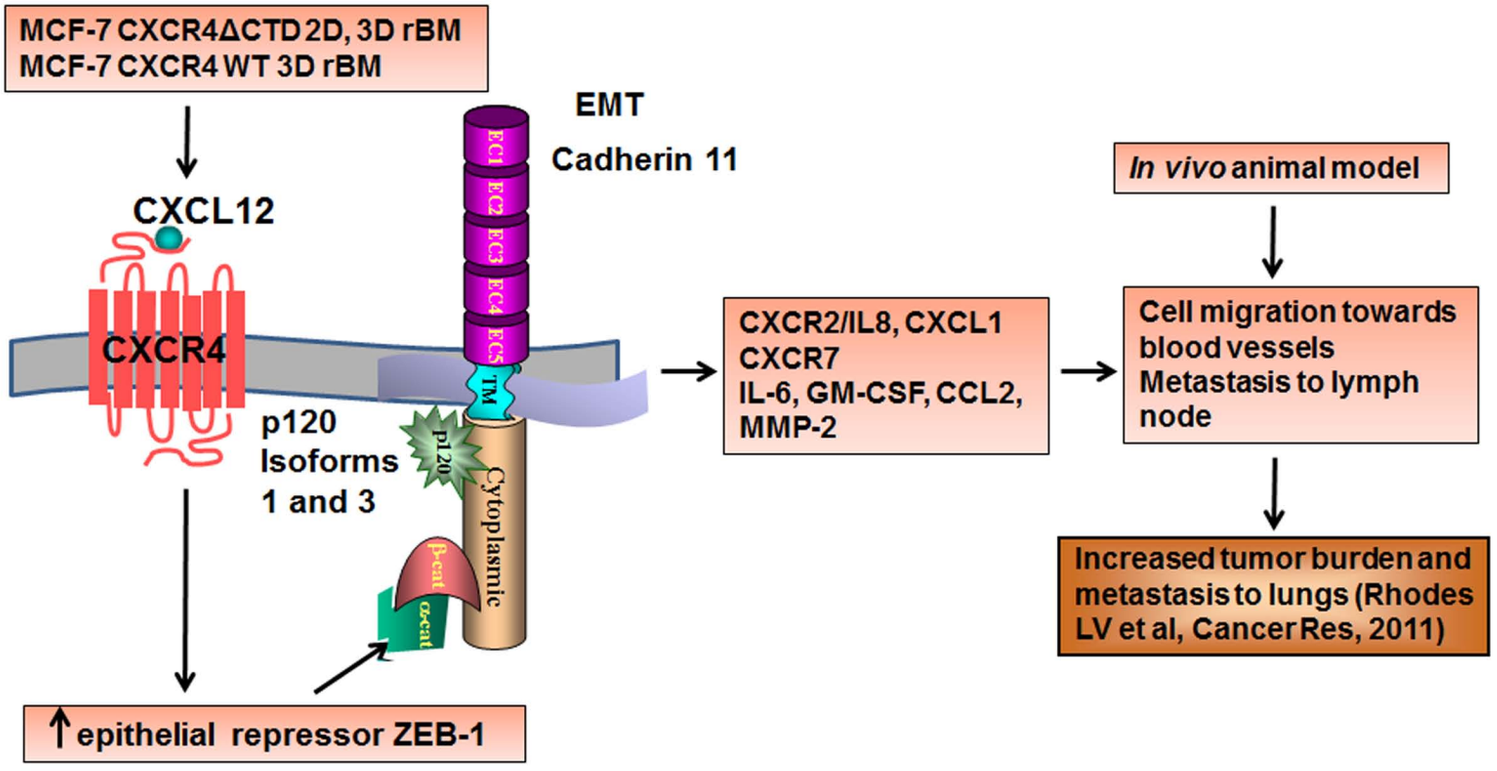

Supplementary Table S1

Pos	Pos	Neg	Neg	ALCAM	ALCAM	Angiopoietin -1	DKK 1	E-cadherin	EGF	EGFR	GRO
Pos	Pos	Neg	Neg	ALCAM	ALCAM	Angiopoietin -1	DKK 1	E-cadherin	EGF	EGFR	GRO
GRO -α	HGF	IFN-gamma	IL-6	MMP-2	MMP-7	MMP-9	NAP -2	SDF-1 α	SDF -1 β	TACE	TGF-β 1
GRO -α	HGF	IFN-gamma	IL-6	MMP-2	MMP-7	MMP-9	NAP -2	SDF-1 α	SDF -1 β	TACE	TGF-β 1
TGF-β 2	Beta cellulin	CCL21	ENA-78	ErbB2	ErbB3	Fractalkine	IGF-I	IL-17	IL-8	CXCL11/ ITAC	Lymphotactin
TGF-β 2	Beta cellulin	CCL21	ENA-78	ErbB2	ErbB3	Fractalkine	IGF-I	IL-17	IL-8	CXCL11/ ITAC	Lymphotactin
MCP -1	NRG1-β1/HRG1- β1	RANTES	TNF-α	VEGF	GCP-2	MIG	S-100b	NEG	NEG	NEG	POS
MCP -1	NRG1-β1/HRG1- β1	RANTES	TNF-α	VEGF	GCP-2	MIG	S-100b	NEG	NEG	NEG	POS